

# Research Progress of Radiolabeled Asn-Gly-Arg (NGR) Peptides for Imaging and Therapy

Molecular Imaging  
Volume 19: 1-11  
© The Author(s) 2020  
Article reuse guidelines:  
sagepub.com/journals-permissions  
DOI: 10.1177/1536012120934957  
journals.sagepub.com/home/mix



Liqin Zhu, MD<sup>1</sup> , Zhikai Ding, MD<sup>1</sup>, Xingliang Li, PhD<sup>2,3</sup>, Hongyuan Wei, PhD<sup>1,2,3</sup>, and Yue Chen, MD<sup>1,3</sup>

## Abstract

Asn-Gly-Arg (NGR) motifs have vasculature-homing properties via interactions with the aminopeptidase N (CD13) expressed on tumor neovasculature. Numerous NGR peptides with different molecular scaffolds have been exploited for targeted delivery of different compounds for imaging and therapy. When conjugated with NGR, complexes recognize the CD13 receptor expressed on the tumor vasculature, which improves the specificity to tumor and avoids systematic toxic reactions. Both preclinical and clinical studies performed with these products suggest that NGR-mediated vascular targeting is an effective strategy for delivering bioactive amounts of cytokines to tumor endothelial cells. For molecular imaging, radiolabeled peptides have been the most successful approach and have been translated into clinic. This review describes current data on radiolabeled tumor vasculature-homing NGR peptides for imaging and therapy.

## Keywords

NGR, radiolabeled, imaging, therapy, tumor

## Introduction

New blood vessels recruit from the preexisting vasculature by neoangiogenesis in the tumor stroma. This is a fundamental process in tumor cell survival, proliferation, and invasion, and it is a multistep process involving growth factors, adhesion molecules, and cellular receptors. Among these, CD13 (also referred to as aminopeptidase N [APN], a zinc-dependent membrane-bound ectopeptidase) is a critical regulator of angiogenesis. CD13 is expressed on activated blood vessels induced by angiogenic signals. The high expression level of CD13 is associated with the progression of tumors, including lung, prostate, and ovarian cancers.<sup>1</sup> Therefore, efforts have been made to identify biomarkers that interact with CD13 expressed in angiogenic vessels to generate new antiangiogenic agents or to obtain ligands for targeted delivery of drugs or imaging agents to tumors.

Asparagine-glycine-arginine (NGR)-containing peptides target the tumor vasculature via interactions with CD13 as seen in peptide-phage library panning in tumor-bearing mice.<sup>2</sup> CD13 is also expressed in normal tissues, including myeloid cells, antigen-presenting cells, mast cells, epithelial cells from renal proximal tubules, small intestine, keratinocytes, prostate, and bile duct canaliculi.<sup>3</sup> However, experiments have

suggested that the NGR-containing peptides can bind CD13-positive vessels in tumors, but not other CD13-rich tissues. This may be due to the expression of different forms of CD13. These results further show the feasibility of using NGR-containing peptides as a potential and promising diagnostic and therapeutic agent.<sup>4</sup> Therefore, numerous efforts have been made to explore the NGR tripeptide motif as vehicle for delivering chemotherapeutic drugs, nanoparticles, and radioisotopes to the tumor. Both the preclinical experiments and clinical trials have shown its utility for imaging the tumor vasculature.<sup>5</sup>

<sup>1</sup> Department of Nuclear Medicine, The Affiliated Hospital, Southwest Medical University, Luzhou, Sichuan, People's Republic of China

<sup>2</sup> Institute of Nuclear Physics and Chemistry, China Academy of Engineering Physics, Mianyang, Sichuan, People's Republic of China

<sup>3</sup> Nuclear Medicine and Molecular Imaging Key Laboratory of Sichuan Province, Luzhou, Sichuan, People's Republic of China

Submitted: 04/12/2019. Revised: 14/04/2020. Accepted: 06/05/2020.

## Corresponding Authors:

Hongyuan Wei and Yue Chen, Department of Nuclear Medicine, The Affiliated Hospital, Southwest Medical University, No 15 Tai Ping St, Jiangyang District, Luzhou, Sichuan 646000, People's Republic of China.

Emails: hywei@caep.cn; chenye5523@126.com



Creative Commons Non Commercial CC BY-NC: This article is distributed under the terms of the Creative Commons Attribution-NonCommercial 4.0 License (<https://creativecommons.org/licenses/by-nc/4.0/>) which permits non-commercial use, reproduction and distribution of the work without further permission provided the original work is attributed as specified on the SAGE and Open Access pages (<https://us.sagepub.com/en-us/nam/open-access-at-sage>).

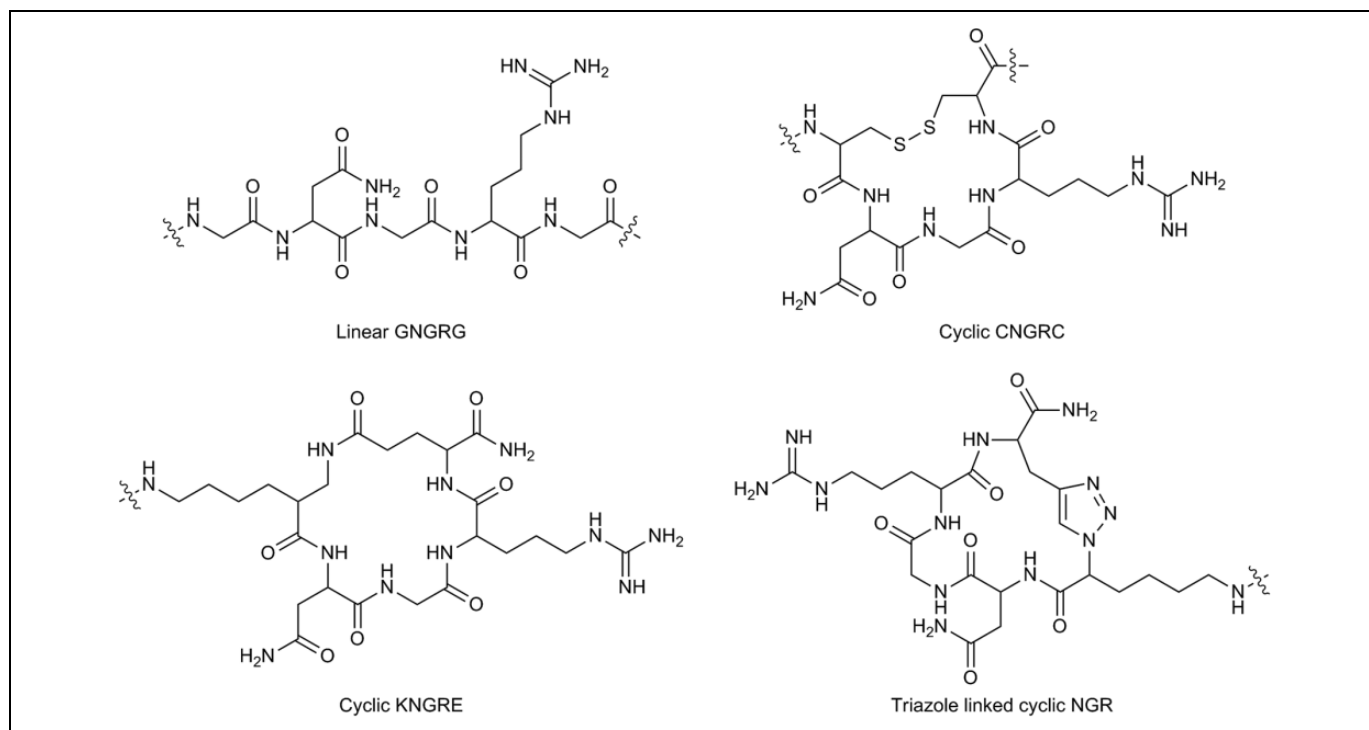


**Figure 1.** Structure of common NGR peptides.

NGR is a promising target for cancer therapy, and it is important to develop an approach for noninvasively imaging CD13 receptor levels in living subjects to identify responsive patients, monitor therapy, and estimate prognosis. NGR-based molecular radioimaging is an optimal method for assessing the expression of CD13 receptor *in vivo* noninvasively and accurately. In this review, we comprehensively summarize the current status of NGR peptide-directed drug delivery and highlight molecular radioimaging in cancer.

## Structures of Common NGR Peptides

Initial reports revealed that a pentapeptide of NGR was sufficient to be the minimum binding motif with an NGR sequence flanked by 1 amino acid at both ends<sup>6</sup> (Figure 1). The results show the different molecular scaffolds of NGR peptides that have been coupled to drugs and particles through the N-terminal or C-terminal.<sup>3,5,7</sup> Although it is generally assumed that all of these peptides could bind to CD13 on the tumor neovasculature, different molecular scaffolds of NGR motifs confer different biochemical and biological properties such as the binding affinity to CD13-positive endothelial cells and different degradation patterns.

Numerous experiments have further confirmed that cyclic NGR (cNGR) displayed stronger affinity and higher specificity toward the CD13 receptors than linear ones.<sup>7,8</sup> First-generation linear forms of the NGR peptides suffered from low selectivity and stability. The improvement and reforming were achieved by developing the cyclic pentapeptides, including NGR cyclized through the disulfide bond (named cCNGRC).<sup>7</sup> To

further improve the stability of NGR toward chemical and enzymatic reactions, more robust cyclizations have been introduced such as the amide linkage made by direct conjugation or the triazole linkage resulting from click chemistry.<sup>8,9</sup> The cNGR ligand, cKNGRE, was cyclized by the amide bond and displayed 3.6-fold greater affinity than linear KNGRG in CD13 cancer cells.<sup>8</sup> When both linear NGR and disulfide-bonded cNGR were coupled with the tumor necrosis factor (TNF)  $\alpha$ , the cNGR-TNF- $\alpha$  exhibited more than 10-fold higher antitumor activity compared to the linear NGR derivative.<sup>7</sup> Except for these, using multimeric cNGR peptides could improve the binding affinity to tumor cells.<sup>10</sup>

Furthermore, the main degradation product of cNGR peptides is characterized by a gain of 1 Da, while the main degradation product of linear NGR is characterized by a loss of 17 Da versus the original peptide. The different degradation patterns of cyclic and linear peptides can be explained by the fact that the disulfide bridge reduces peptide bond flexibility and decreases the potential reactivity of the  $\alpha$ -amino group with the Asn side chain or with the succinimide intermediate.<sup>11</sup> The Asn residue of linear NGR tends to spontaneously deamidate and generate Asp and isoAsp residues.<sup>12</sup> This reaction occurs by nucleophilic attack of the backbone amino-group on the Asn side chain, leading to the formation of mixtures of isoDGR and DGR with changes in peptide bond length and charge. As a consequence, the change in NGR to isoDGR/DGR caused a loss of CD13-binding affinity and gain of  $\alpha_v\beta_3$ -integrin-binding activity.<sup>12</sup>

Considering the biochemical and biological characteristics of different molecular scaffolds such as peptide stability and

receptor binding specificity, NGR drug conjugates and fusion proteins should be carefully designed, produced, stabilized, and developed to further stimulate investigation.

## NGR Peptide-Based Drug Delivery Systems

Due to their neovasculature homing properties, NGR peptides have been exploited for targeted delivering of different compounds to tumors including cytokines, chemotherapeutic drugs, liposomes, antiangiogenic agents, imaging agents, and nucleic acid to CD13-positive tumor neovasculature.<sup>3</sup> NGR-based chemotherapeutic agents such as NGR-liposomal doxorubicin, docetaxel-loaded polymeric micelles, platinum (IV), carboplatin, 5-fluorouracil prodrug, and 5-fluoro-2'-deoxyuridine prodrug showed selectively toxicity for angiogenic endothelial cells and anticancer activity in mice.<sup>13,14</sup> NGR-based cytokines such as tumor necrosis factor  $\alpha$  (hTNF $\alpha$ ), interferon- $\gamma$  (IFN $\gamma$ ), IFN  $\alpha$ 2a, endostatin, a tumstatin fragment 35-135, and truncated tissue factor also have antiangiogenic activity.<sup>3,15-17</sup>

Of these, NGR-based tumor necrosis factor  $\alpha$  (NGR-hTNF) is the most widely studied molecule. It has been studied in phase I-III clinical trials.<sup>18</sup> Tumor necrosis factor  $\alpha$ , an inflammatory cytokine, was initially identified for its impressive antitumor activity in a variety of tumors. It destroys tumor-associated vessels and activates the immunogenic response rather than by directly damaging tumors. However, despite the significant antitumor effects observed in animal models, phase I-II clinical trials showed that TNF induced toxic effects and extremely low antitumor activity.<sup>19</sup> Tumor necrosis factor combined with NGR had stronger antitumor activity and less toxicity than TNF alone. The dose-response curve showed microgram doses of TNF were necessary to induce antitumor effects, while a wider range of NGR-TNF doses (from picograms to micrograms) showed antitumor activity.<sup>19</sup>

A phase I study (EORTC 16041) investigated dose-limiting toxicities, maximum tolerated dose (MTD), pharmacodynamics, pharmacokinetics, and vascular response in solid tumors. Here, NGR-hTNF were administered within 20 or 60 minutes in the range of 0.2 to 60 g/m<sup>2</sup>. The MTD was 45 g/m<sup>2</sup> when administered in 1 hour, and the most frequently observed toxicities were chills and fever.<sup>20</sup> A later phase I study defined the optimal biological dose of NGR-hTNF to be 0.8 g/m<sup>2</sup> in the low dose range (0.2-1.6 g/m<sup>2</sup>, 1-hour infusion).<sup>21</sup> A randomized, double-blind, placebo-controlled phase 3 trial has been conducted to investigate its efficacy and safety in patients with malignant pleural mesothelioma who progressed during or after the first-line treatment: 200 patients were selected to receive NGR-hTNF plus best investigator choice and 200 patients received placebo plus best investigator choice. Although the overall survival did not differ between the NGR-hTNF group and the placebo group (median: 8.5 months, 95% CI: 7.2-9.9 vs 8.0 months, 95% CI: 6.6-8.9;  $P = .58$ ), subgroup analyses suggest patients with shorter treatment intervals may benefit from NGR-hTNF.<sup>22</sup> In addition, NGR-hTNF has been performed on hepatocellular carcinoma (HCC), malignant pleural mesothelioma (MPM), metastatic melanoma, small cell lung

cancer, relapsed ovarian cancer, and colorectal cancer (CRC) both alone and in combination with chemotherapy in different phases of clinical trials. All these studies showed that NGR-hTNF was well tolerated with significant disease control at low dose.<sup>22-27</sup> Thus, NGR-hTNF deserves further investigation in MPM, HCC, and CRC. These findings suggest an improved antitumor activity by the NGR-mediated vascular targeting approach.

## Monomeric Compounds of NGR for Tumor Radioimaging

Different NGR motifs have been labeled with different radio-nuclides through different bifunctional chelators. The most studied nuclides were <sup>68</sup>Ga and <sup>64</sup>Cu for positron emission tomography (PET) imaging and <sup>99m</sup>Tc for single-photon emission computed tomography (SPECT) imaging. Positron emission tomography provides higher spatial resolution than SPECT.

Zhang et al<sup>28</sup> investigated the feasibility of <sup>68</sup>Ga-labeled linear NGR for the detection of the CD13-positive tumors. MicroPET imaging showed high focal accumulation of <sup>68</sup>Ga-DOTA-NGR visualized at the tumor site at 1 hour in A549 tumor xenografts. The maximum uptake of <sup>68</sup>Ga-DOTA-NGR in A549 tumors was nearly 1% ID/g, and the maximum tumor/lung ratios were  $12.58 \pm 1.26$  at 1.5 hours. Immunohistochemistry confirmed that radioactivity was correlated with expression of CD13 in A549 xenografts and confirmed that NGR is a promising molecular probe for CD13. Although tumor uptake was higher than the APN-negative MDA-MB231 tumor group, the tumor uptake of <sup>68</sup>Ga-labeled linear NGR is not optimal for tumor radioimaging. While <sup>18</sup>F-fluorodeoxyglucose PET/computed tomography (CT) is effective for early detection in various malignant diseases, it was limited in detecting well-differentiated HCCs. This may be caused by the overexpressed glucose-6-phosphatase (G6Pase) and the low expressed glucose transporter 1.<sup>29</sup> In terms of the high expression rate of CD13 in a variety of HCC cell lines, Gao et al<sup>30</sup> compared <sup>68</sup>Ga-DOTA-G3-cNGR (cycled by disulfide bond) and <sup>18</sup>F-FDG to image well-differentiated SMMC-7721 HCC xenografts (positive for both CD13 and G6Pase). The extra 3 glycines were added to protect the core motif NGR and increase peptide half-life and stability. In vivo microPET/CT imaging studies indicated the uptake of <sup>68</sup>Ga-DOTA-G3-cNGR in SMMC-7721 tumors was similar to that in the CD13-positive control HT-1080 tumors ( $2.17\% \pm 0.21\%$  ID/g vs  $2.46\% \pm 0.23\%$  ID/g,  $P = .18 > .05$ ) and was obviously higher than that in the CD13-negative control HT-29 malignancy ( $2.17\% \pm 0.21\%$  ID/g vs  $0.67\% \pm 0.20\%$  ID/g,  $P = .0148 < .05$ ). The uptake of <sup>68</sup>Ga-DOTA-G3-cNGR in SMMC-7721-derived tumors was 2.97-fold higher than that of <sup>18</sup>F-FDG ( $2.17\% \pm 0.21\%$  ID/g vs  $0.73\% \pm 0.26\%$  ID/g). The tumor/liver ratio of <sup>68</sup>Ga-DOTA-G3-cNGR was 2-fold higher than that of <sup>18</sup>F-FDG in the SMMC-7721 HCC models. In terms of high uptake and T/L ratio in well-differentiated HCC tumor, <sup>68</sup>Ga-DOTA-G3-cNGR was more suitable for imaging well-

differentiated HCC as compared to  $^{18}\text{F}$ -FDG. As compared to the linear  $^{68}\text{Ga}$ -DOTA-NGR studied by Zhang et al., the circular structure indeed significantly improves the uptake of tumors.<sup>28</sup>

Although there are multiple studies using DOTA as a chelator for  $^{68}\text{Ga}$ ,  $^{68}\text{Ga}$ -NOTA system has been shown to have higher stability than that of  $^{68}\text{Ga}$ -DOTA system.<sup>31</sup> Shao et al.<sup>32</sup> developed  $^{68}\text{Ga}$ -NOTA-G3-cNGR for noninvasive imaging of CD13 expression in vivo by PET. The disulfide bond cycled cNGR radioprobe exhibited rapid and significant tumor uptake and good tumor-to-background contrast in a subcutaneous HT-1080 fibrosarcoma mouse model. HT-1080 tumor uptake of  $^{68}\text{Ga}$ -NOTA-G3-NGR was  $6.30\% \pm 2.27\%$ ,  $5.03\% \pm 1.95\%$ , and  $3.84\% \pm 2.32\%$  ID/g at 0.5, 1, and 2 hours, respectively. The ratios of HT-1080 tumor uptake to muscle, liver, kidney, and blood at 1 hours were  $7.39 \pm 2.20$ ,  $3.14 \pm 0.35$ ,  $0.57 \pm 0.02$ , and  $4.78 \pm 1.14$ , respectively. Versus uptake of  $^{68}\text{Ga}$ -DOTA-G3-cNGR studied by Gao et al.<sup>30</sup> in HT-1080 tumors,  $^{68}\text{Ga}$ -NOTA-G3-cNGR shows significantly higher uptake ( $6.30\% \pm 2.27\%$  ID/g vs  $2.46\% \pm 0.23\%$  ID/g) in HT-1080 tumor and higher tumor/muscle ratios ( $7.39 \pm 2.20$  vs  $2.14 \pm 0.43$ ), suggesting better chelation of  $^{68}\text{Ga}$ -NOTA system.

Poor uptake and short retention time due to the smaller molecular weight are the most common problems for small-molecule peptide probes.<sup>33</sup> The most important reason for the short half-life time of peptides and proteins is their rapid renal excretion and enzymatic degradation. In general, molecules with a mass below 5 kDa are not bound to plasma proteins and could be completely excreted through renal pathways. Molecules with a mass greater than 50 kDa cannot be found in the glomerular ultrafiltrate. Zhao et al.<sup>34</sup> introduced CendR into the NGR peptide (denoted as iNGR) and then compared the efficacy of  $^{68}\text{Ga}$ -DOTA-iNGR and  $^{68}\text{Ga}$ -DOTA-NGR (cycled by disulfide bond) as a new molecular probe for microPET imaging of CD13-positive xenografts. The CendR motif (R/KXXR/K), a C-terminal sequence containing a C-terminal arginine or lysine with a free carboxyl group, can increase the residence time, increase the flow of the peptide through blood vessels, and direct the peptide to pass through biological barriers by interacting with neuropilin-1 (NRP-1).<sup>35</sup> In vivo microPET imaging studies showed that the tumor uptake values were  $3.41 \pm 0.28$ ,  $2.97 \pm 0.30$ , and  $2.64 \pm 0.31\%$  ID/g at 0.5, 1, and 1.5 hours for  $^{68}\text{Ga}$ -DOTA-iNGR and  $2.68 \pm 0.35$ ,  $1.91 \pm 0.32$ , and  $1.45 \pm 0.30\%$  ID/g for  $^{68}\text{Ga}$ -DOTA-NGR, respectively ( $P < .05$ ). The maximum uptake rate of  $^{68}\text{Ga}$ -DOTA-iNGR in HT-1080 cells was about 2-fold higher than  $^{68}\text{Ga}$ -DOTA-NGR ( $1.78\% \pm 0.14\%$  vs  $0.90\% \pm 0.12\%$ ) at 2 hours. Furthermore, the uptake rate of  $^{68}\text{Ga}$ -DOTA-iNGR was similar to that of  $^{68}\text{Ga}$ -DOTA-NGR after being blocked by NRP-1 antibody. Tumor uptake of  $^{68}\text{Ga}$ -DOTA-iNGR could be completely blocked by cold NGR and partially blocked by neutralizing NRP-1 antibody, indicating that the enhancement was attributed to the interaction of CendR and NRP-1. The uptake of  $^{68}\text{Ga}$ -DOTA-iNGR in HT-1080 tumors was significantly higher than that of  $^{68}\text{Ga}$ -DOTA-NGR at all time points

and with longer retention time. The CendR motif modification is a promising method for improving NGR peptide performance.

In addition to radionuclide  $^{68}\text{Ga}$  for PET imaging,  $^{99\text{m}}\text{Tc}$  has been used to label NGR peptides for SPECT. NGR peptide (cyclic via a disulfide bond) was synthesized and directly labeled with  $^{99\text{m}}\text{Tc}$  and then subjected to SPECT imaging of CD13 expression in a CD13 receptor-positive HepG2 hepatoma xenograft mouse model. A SPECT imaging also showed significant uptake in tumor and dominant renal and hepatic clearance. The highest tumor uptake of  $^{99\text{m}}\text{Tc}$ -cNGR was  $3.26\% \pm 0.63\%$  ID/g, with the highest tumor-to-normal tissue (T/NT) ratio  $7.58 \pm 1.92$  at 8 hours. However, the tumor/liver at 1 hour was  $0.63 \pm 0.33$ , which could limit applications in abdominal diseases.<sup>36</sup> NGR peptides could be conjugated with the most commonly used bifunctional technetium chelators mercaptoacetylglucylglycylglycine (MAG3). Faintuch et al.<sup>37</sup> evaluated the in vitro and in vivo performance of  $^{99\text{m}}\text{Tc}$  radiolabeled pegylated cNGR peptide  $^{99\text{m}}\text{Tc}$ -MAG3-PEG8-cNGR (cycled through the amide bond) as a marker of imaging angiogenesis in lung (A549), prostate (PC-3), and ovarian (OVCAR-3) tumors. PEGylation protects peptides from enzymatic degradation and enhances overall hydrophilicity of the compounds. This increases the peptide half-life and stability and decreases immunogenicity. Lung and ovarian cancer cells show promising results, but prostate cancer cells do not. This may be caused by the different receptor expression levels in tumor cells.

Glutamic acid-cysteine-glycine (ECG) is a tripeptide containing a sulfur and multiple nitrogen atoms. It shows strong chelation ability with  $^{99\text{m}}\text{Tc}$ .<sup>38</sup> Through using peptides ECG as bifunctional coupling agent, Kim et al.<sup>39</sup> developed 2 NGR-containing hexapeptides, ECG-NGR and NGR-ECG, as molecular imaging agents to target APN/CD13 in HT-1080 fibrosarcoma. The tumor/muscle uptake ratio of  $^{99\text{m}}\text{Tc}$ -ECG-NGR reached  $5.7 \pm 0.4$  at 4 hours, which is comparable to dimeric NGR-based peptides  $^{99\text{m}}\text{Tc}$ -NGR<sub>2</sub> in HepG2 hepatoma xenografts model ( $6.06$  at 4 hours).<sup>40</sup> In contrast, the tumor/muscle uptake ratio of  $^{99\text{m}}\text{Tc}$ -NGR-ECG was only  $2.9 \pm 0.5$  at 4 hours, which is lower than that of  $^{99\text{m}}\text{Tc}$ -ECG-NGR. In vitro and in vivo studies showed that  $^{99\text{m}}\text{Tc}$ -ECG-NGR has a better specific binding ability for the tumor cells and tumor tissue than  $^{99\text{m}}\text{Tc}$ -NGR-ECG. This may be because the asparagine residue of NGR-ECG is not protected by other amino acids and could be easily deamidated by a nucleophilic attack. A series reaction after nucleophilic attack of the backbone NH center on the asparagine side chain leads to the formation of mixtures of isoDGR/DGR, which lead to a loss of CD13-binding affinity and lower tumor uptake.<sup>11,12</sup> We concluded that different molecular scaffolds have a significant influence on peptide-binding properties of APN/CD13 in tumor neovasculature. Modification of the N-terminus seems crucial to improving the in vitro and in vivo performance of NGR peptides.

Chlorambucil (CLB), a DNA-alkylating nitrogen mustard, is widely used to treat chronic lymphocytic leukemia, lymphomas, breast, and ovarian carcinoma and a variety of other solid tumors. To address the systemic toxicity and various other side

effects caused by its low specificity, Vats K et al<sup>41</sup> explored the targeted chemotherapy ability of CLB-cNGR and used <sup>99m</sup>Tc to monitor its pharmacokinetics and biodistribution through the chelator 6-hydra-zinonicotinic acid (HYNIC). Drugs conjugated with the targeting vectors NGR peptides can act as conduits for site-specific delivery and can then overcome the nonspecific accumulation in normal tissues.<sup>42</sup> The cytotoxicity studies demonstrated that CLB-cNGR significantly inhibits B16F10 cell growth at all concentrations versus CLB or cNGR. A ~25-fold excess concentration of CLB could achieve similar cytotoxicity as CLB-cNGR. In vivo biodistribution studies showed that the maximum tumor uptake was  $2.45\% \pm 0.28\%$  ID/g at 30 minutes and maximum tumor to muscle ratio was  $4.23 \pm 0.57$  at 180 minutes in C57BL6 mice bearing melanoma tumors. This suggests that the systemic exposure and side effects of drugs can be reduced by conjugation to the targeting peptide. In addition, radiolabeled peptide drug conjugates contribute can help track the pharmacokinetics of the drug. In general, <sup>99m</sup>Tc-labeled NGR peptides have similar tumor uptake as <sup>68</sup>Ga but also have higher liver uptake, which limits their use in abdominal diseases.

## Dimeric Compounds of NGR for Tumor Radioimaging

Although most NGR peptide-based probes can target tumors by binding to the CD13 receptor, they usually show moderate tumor uptake and unfavorable pharmacokinetics, which limit their applications in tumor imaging and therapy. Dimerization of a ligand can be an effective approach to enhance the binding affinity to specific receptor leading to higher tumor uptake through multivalency effects (multivalency effects refer to the synthesis of more than one targeting ligand in a single reagent to simultaneously bind multiple receptors and enhance the overall binding affinity).<sup>43</sup>

The most common multivalent system is the dimer. It has been reported that dimeric RGD peptides can markedly improve the binding affinity of the RGD ligand to integrin  $\alpha_v\beta_3$  receptor.<sup>43</sup> CD13 receptor and integrin  $\alpha_v\beta_3$  receptors are both cell surface targets of tumor angiogenesis: Dimeric NGR peptides with 2 repeating cNGR may also lead to higher affinity of the receptor and uptake in the tumor. The increased molecular size can prolong circulation time, reduce tumor washout rate, and lead to longer retention time in the tumor.

<sup>64</sup>Cu-labeled monomeric and dimeric NGR peptides (cycled by disulfide bond) for microPET imaging of CD13 receptor expression have also been explored. The HT-1080 tumor uptake was  $3.33\% \pm 0.10\%$ ,  $3.09\% \pm 0.20\%$ ,  $2.32\% \pm 0.17\%$ , and  $1.79\% \pm 0.27\%$  ID/g at 1, 2, 4, and 24 hours for <sup>64</sup>Cu-DOTA-NGR<sub>1</sub>; the corresponding values were  $6.53\% \pm 0.20\%$ ,  $6.09\% \pm 0.18\%$ ,  $5.22\% \pm 0.17\%$ , and  $3.60\% \pm 0.23\%$  ID/g at 1, 2, 4, and 24 hours, respectively, for <sup>64</sup>Cu-DOTA-NGR<sub>2</sub>. The tumor to muscle ratio at 4 hours was calculated to be  $3.91 \pm 0.19$ , while the corresponding values for <sup>64</sup>Cu-DOTA-NGR<sub>2</sub> were  $7.57 \pm 0.15$  (Figure 2). Both the cell-based binding assay and microPET imaging suggested a nearly 2-fold higher CD13 avidity of <sup>64</sup>Cu-

DOTA-NGR<sub>2</sub> than the corresponding monomeric <sup>64</sup>Cu-DOTA-NGR<sub>1</sub> in HT-1080 cells. Both <sup>64</sup>Cu-DOTA-NGR<sub>1</sub> and <sup>64</sup>Cu-DOTA-NGR<sub>2</sub> showed predominant uptake in liver and kidneys at all time points.<sup>44</sup> High accumulation and retention in the liver may result from the slow dissociation of <sup>64</sup>Cu from the DOTA chelator. The instability of <sup>64</sup>Cu-DOTA can lead to de-metalation and subsequent accumulation in nontarget tissues and organs such as in the liver. This is a common problem for <sup>64</sup>Cu-DOTA probes. Except for trapping of <sup>64</sup>Cu in the mouse liver, another important reason for liver uptake may be caused by CD13 expression in mouse liver. Thus, characterizing the CD13 expression levels in normal organs and tissues, such as in liver and kidneys, will promote clinical imaging applications of NGR-containing probes.

In other research, a <sup>64</sup>Cu-labeled dimeric disulfide bond with a cNGR peptide based on the sarcophagine cage has been studied to decrease Cu<sup>2+</sup> dissociation. The sarcophagine cage (denoted as “Sar”) is a macrocyclic chelator. Although it has excellent binding ability and a higher radiolabeling efficiency for <sup>64</sup>Cu<sup>2+</sup> than other chelators, it has also failed to address the problem of significant uptake in liver in this study. The liver uptake values were calculated to be  $9.81\% \pm 0.62\%$  ID/g at 1 hour; the ratio of HT-1080 tumor uptake to liver at 4 hours was  $0.79 \pm 0.27$ , which is comparable to the value of <sup>64</sup>Cu-DOTA-NGR<sub>2</sub>.<sup>44</sup> The cell-based binding assay, microPET imaging, and biodistribution studies indicated that <sup>64</sup>Cu-Sar-NGR<sub>2</sub> has a similar CD13 affinity and comparable biodistribution as previously reported as <sup>64</sup>Cu-DOTA-NGR<sub>2</sub>. This confirmed that the multimerization of NGR peptides enhances CD13-binding affinity.<sup>44,45</sup>

Another study was carried out to compare <sup>99m</sup>Tc-labeled monomeric and dimeric linear NGR peptides NGR<sub>1</sub> and NGR<sub>2</sub> for SPECT imaging of CD13 expression in HepG2 hepatoma xenografts. Similar to <sup>64</sup>Cu-labeled monomeric and dimeric NGR peptides, the dimeric <sup>99m</sup>Tc-NGR<sub>2</sub> exhibited overall better properties in vitro and in vivo versus the monomeric <sup>99m</sup>Tc-NGR<sub>1</sub> in terms of binding avidity, cellular uptake, tumor uptake and retention, tumor to background contrast ratio, and pharmacokinetics. However, <sup>99m</sup>Tc-NGR<sub>1</sub> and <sup>99m</sup>Tc-NGR<sub>2</sub> both showed significant liver uptake:  $15.87\% \pm 1.76\%$  ID/g for <sup>99m</sup>Tc-NGR<sub>2</sub> and  $10.30\% \pm 1.32\%$  ID/g for <sup>99m</sup>Tc-NGR<sub>1</sub> at 1 hour; this indicates that they are not suitable for abdominal tumors.<sup>40</sup>

In terms of tumor uptake and tumor/muscle ratio, dimeric compounds demonstrated better pharmacokinetics with a higher tumor to nontarget ratio versus the corresponding monomeric. Although <sup>64</sup>Cu- and <sup>99m</sup>Tc-labeled NGR peptides have obvious tumor uptake, they both suffered from significant liver uptake. <sup>68</sup>Ga-labeled dimeric compounds discussed next could be the most ideal radioactive probes. They can reduce the liver uptake with comparable tumor uptake with <sup>64</sup>Cu- and <sup>99m</sup>Tc-labeled NGR peptides.

## Comparative Experiments of NGR and RGD-Based Radioimaging

Among the various peptides identified by phage-display to target the tumor vessels in a mouse model, 2 peptide motifs

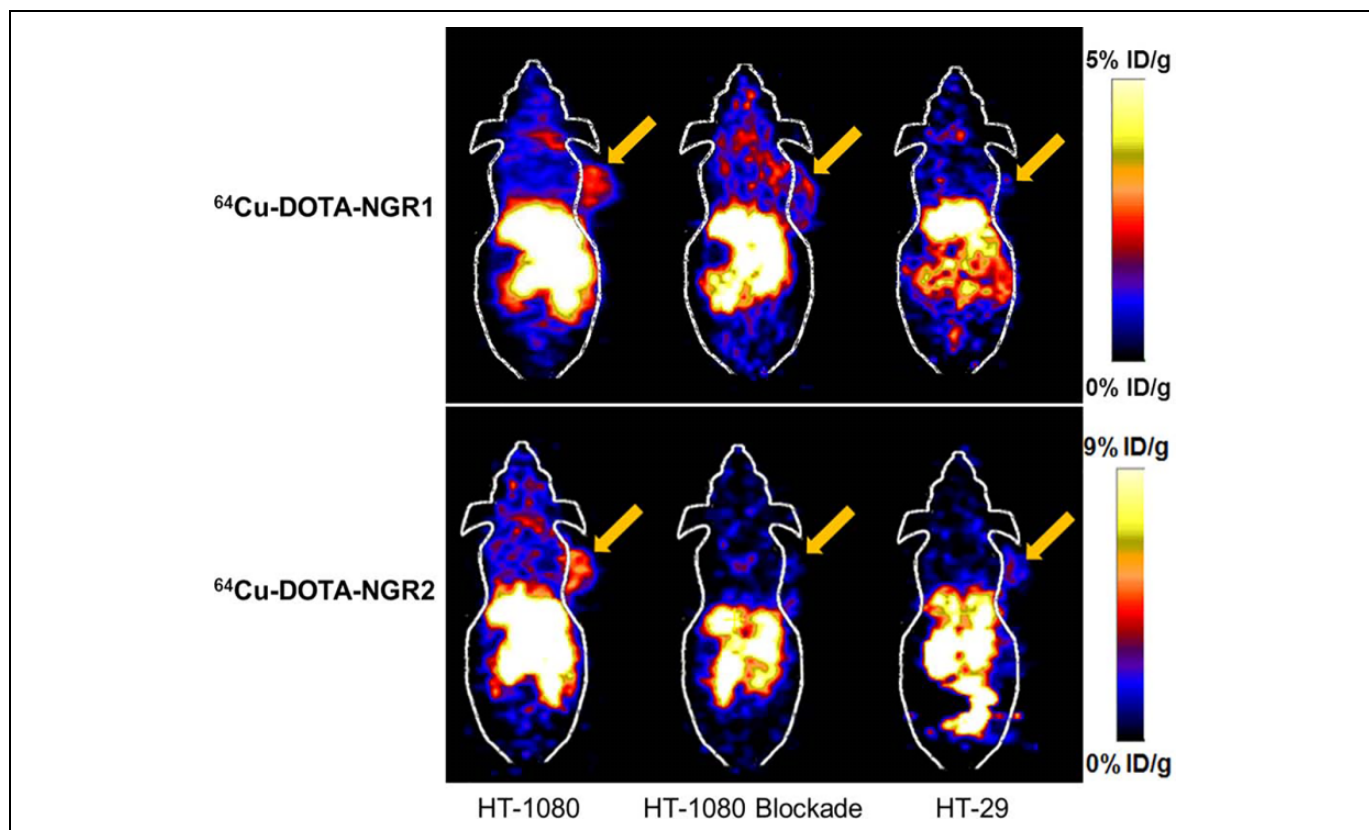


**Figure 2.** Representative micro positron emission tomography images of mice bearing HT-1080 or HT-29 tumors. Right front flank images shown 4 hours after intravenous (IV) administration of  $^{64}\text{Cu}$ -DOTA-NGR1 or  $^{64}\text{Cu}$ -DOTA-NGR2. The blocking study was performed by IV injection of  $^{64}\text{Cu}$ -DOTA-NGR1 or  $^{64}\text{Cu}$ -DOTA-NGR2 with coinjection of NGR peptide [c(CNGRC)] in HT-1080 tumor xenografts. It suggested a nearly 2-fold higher CD13 avidity of  $^{64}\text{Cu}$ -DOTA-NGR2 than the corresponding monomeric  $^{64}\text{Cu}$ -DOTA-NGR1 in HT-1080 cells. Adapted with permission from Kai Chen et al.<sup>44</sup> Copyright (2019) America Chemical Society.

have been well characterized with known recognition sites. One of them contains the sequence Asn-Gly-Arg (NGR) and was found to bind the CD13 receptor isoform upregulated in the tumor vasculature. Another peptide contains the sequence Arg-Gly-Asp (RGD) and specifically recognizes the upregulated  $\alpha_v\beta_3$  and  $\alpha_v\beta_5$  integrins in tumor endothelial cells.<sup>46</sup> Both RGD and NGR tripeptide motifs have been explored as vehicles for delivering chemotherapeutic drugs, radioisotopes, and nanoparticles to angiogenic tumors. There are numerous studies into RGD-radiolabeled peptides such as SPECT isotope  $^{99\text{m}}\text{Tc}$  and PET with  $^{18}\text{F}$ ,  $^{64}\text{Cu}$ , and  $^{68}\text{Ga}$ ; however, there are few reports on  $^{68}\text{Ga}$ - and  $^{64}\text{Cu}$ -labeled NGR peptides so far. Although the NGR peptide shows higher selectivity toward tumor cells and has a 3-fold higher specificity than the RGD peptides, several direct comparisons between radiolabeled NGR and RGD peptides have different conclusions.<sup>43,47</sup>

Shao et al.<sup>46</sup> directly compared  $^{68}\text{Ga}$ -NOTA-G3-NGR<sub>2</sub> and  $^{68}\text{Ga}$ -NOTA-G3-RGD<sub>2</sub> probes for imaging tumor angiogenesis in HT-1080 tumor xenografts coexpressing high levels of CD13 and  $\alpha_v\beta_3/\alpha_v\beta_5$  integrin. The linker and chelator remained the same. RGD was cyclized by the amino group (N-terminus of phenylalanine) with the carboxyl branch in lysine residue; the cyclization of CNGRC used a disulfide bridge. Figure 3

shows no significant difference between the 2 probes in terms of tumor uptake based on microPET imaging ( $7.84\% \pm 1.94\%$  ID/g for  $^{68}\text{Ga}$ -NOTA-G3-RGD<sub>2</sub> vs  $6.42\% \pm 2.21\%$  ID/g for  $^{68}\text{Ga}$ -NOTA-G3-NGR<sub>2</sub> at 0.5 hour); the tumor/muscle ratio was  $8.12 \pm 1.69$  for  $^{68}\text{Ga}$ -NOTA-G3-RGD<sub>2</sub> vs  $7.76 \pm 1.16$  for  $^{68}\text{Ga}$ -NOTA-G3-NGR<sub>2</sub>.<sup>46</sup> The liver uptake of  $^{68}\text{Ga}$ -NOTA-G3-NGR<sub>2</sub> and  $^{68}\text{Ga}$ -NOTA-G3-RGD<sub>2</sub> were  $2.33\% \pm 0.42\%$  and  $2.94\% \pm 0.35\%$  ID/g at 0.5 hour, and the tumor to liver ratio of HT-1080 was  $3.47 \pm 0.69$  for  $^{68}\text{Ga}$ -NOTA-G3-NGR<sub>2</sub> and  $3.26 \pm 1.23$  for  $^{68}\text{Ga}$ -NOTA-G3-RGD<sub>2</sub> at 1 hour. The liver accumulation of  $^{68}\text{Ga}$ -NOTA-G3-NGR<sub>2</sub> and  $^{68}\text{Ga}$ -NOTA-G3-RGD<sub>2</sub> was significantly lower than previously reported for  $^{64}\text{Cu}$ - or  $^{99\text{m}}\text{Tc}$ -labeled NGR peptides.<sup>40,44,45</sup> This result suggests that these 2 probes can be an alternative for PET imaging in patients with fibrosarcoma.

Another study compared  $^{68}\text{Ga}$ -NOTA-cNGR and  $^{68}\text{Ga}$ -NODAGA-c(RGD)<sub>2</sub> in subcutaneously injected and subrenal (SRCA) implanted mesoblastic nephroma (NeDe) tumor cells but with different conclusions.<sup>48</sup> In contrast to Shao et al.,<sup>46</sup> this study selected c[KNGRE]-NH<sub>2</sub>(cyclic(lysine-asparagine-glycine-arginine-glutamic acid amide)) cyclic peptides because the cNGR peptides with a succinimide ring closure are more stable and can prevent deamidation versus the disulfide-



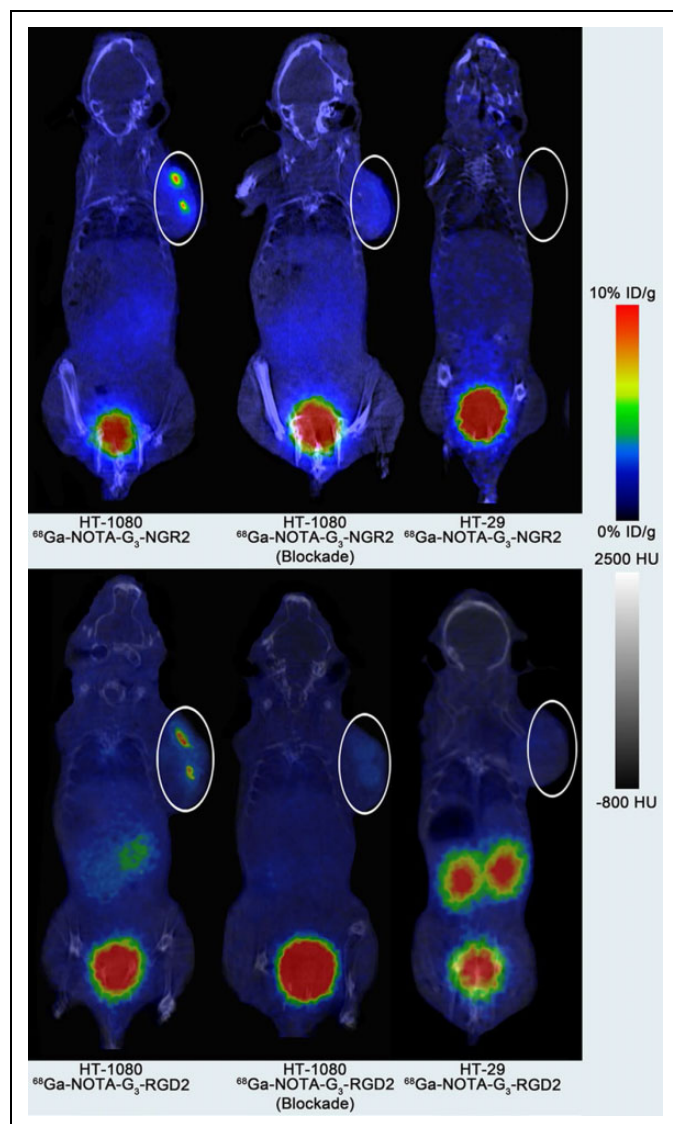


**Figure 3.** Representative image of mice bearing HT-1080 or HT-29 tumors after intravenous administration of  $^{68}\text{Ga}$ -NOTA-G3-NGR2 or  $^{68}\text{Ga}$ -NOTA-G3-RGD2 at 1 hour postinjection, and the coinjection of nonlabeled NOTA-G3-NGR2 or NOTA-G3-RGD2 as blocking agents. Tumors are indicated using circles. There is no significant difference between the 2 probes in terms of tumor uptake based on micro positron emission tomography imaging. Adapted with permission from Yahui Shao et al.<sup>46</sup> Copyright (2019) America Chemical Society.

bridged cNGR. Although there was no significant increase in mean standardized uptake value ( $\text{SUV}_{\text{mean}}$ ) ( $1.73 \pm 0.39$  for  $^{68}\text{Ga}$ -NOTA-cNGR and  $1.31 \pm 0.24$  for  $^{68}\text{Ga}$ -NODAGA-c(RGD)<sub>2</sub>, respectively), the  $\text{SUV}_{\text{max}}$  and T/M  $\text{SUV}_{\text{max}}$  of  $^{68}\text{Ga}$ -NOTA-cNGR were nearly 2-fold higher than  $^{68}\text{Ga}$ -NODAGA-c(RGD)<sub>2</sub> in NeDe tumor-bearing rats with a subcutaneous tumor model ( $11.47 \pm 1.37$  and  $12.47 \pm 2.19$  for  $^{68}\text{Ga}$ -NOTA-cNGR and  $4.96 \pm 0.47$  and  $6.98 \pm 0.55$  for  $^{68}\text{Ga}$ -NODAGA-c(RGD)<sub>2</sub>). In summary, this study revealed that  $^{68}\text{Ga}$ -NOTA-cNGR performs better than dimeric RGD

tracers in NeDe tumor cell lines. This might be due to the differences in the structure and stability of the cNGR peptides.<sup>48</sup>

$^{99\text{m}}\text{Tc}$ -MAG<sub>3</sub>-PEG<sub>8</sub>-cRGD and  $^{99\text{m}}\text{Tc}$ -MAG<sub>3</sub>-PEG<sub>8</sub>-cNGR (both were cyclic PEGylated pentapeptides) were compared in a SKMEL28 melanoma model and B16F10 melanoma model for angiogenesis detection.<sup>49</sup> RGD performs better than NGR in SKMEL28 human melanoma-bearing mice in terms of tumor uptake, tumor/blood ratio, and tumor/muscle ratio; the difference was not remarkable in B16F10 human melanoma-bearing mice. The structure of the targeted peptides influences the performance of radiotracers, and this experiment suggested that expression level of the markers in different cells also has a greater impact.

Rapid radiometallation kinetics at low concentration and ambient temperature make *N*, *N'*-bis-[2-hydroxy-5-(carboxyethyl)benzyl]ethylenediamine-*N*, *N'*-diacetic acid (HBED-CC) an attractive chelator for  $^{68}\text{Ga}$  radiolabeling. Therefore, Satpati D<sup>50</sup> investigated the potential of  $^{68}\text{Ga}$ -HBED-CC-cNGR (cyclized by the disulfide bond) and  $^{68}\text{Ga}$ -HBED-CC-cRGD as tumor targeting radiotracers. The  $^{68}\text{Ga}$ -HBED-CC-cRGD displayed higher specificity in integrin  $\alpha_v\beta_3$ -positive B16F10 cells and higher uptake in B16F10 tumors versus  $^{68}\text{Ga}$ -HBED-CC-cNGR; the 2 radiotracers exhibited similar uptake in HT-1080 tumor xenografts. In terms of the tracer uptake in HT-1080 tumors,  $^{68}\text{Ga}$ -NOTA-G3-cNGR ( $5.03\% \pm 1.95\%$  ID/g at 1 hour)<sup>32</sup> and  $^{64}\text{Cu}$ -DOTA-NGR ( $3.33\% \pm 0.10\%$  ID/g at 24 h)<sup>44</sup> show higher retention in HT-1080 tumors than  $^{68}\text{Ga}$ -HBED-CC-c(NGR) ( $1.5\% \pm 0.1\%$  ID/g at 1 hour). This may be due to different chelators and the absence of a spacer (3 glycine units) in the  $^{68}\text{Ga}$ -HBED-CC-cNGR radiotracer.<sup>50</sup>

These experiments show that different tumors with different expression levels of CD13 are best imaged with different structures of peptides and chelating agents. They can dramatically affect tumor uptake.

## NGR-Based Radiopharmaceuticals for Tumor Therapy

NGR-based peptides can specifically bind to overexpressed CD13 receptor in angiogenic blood vessels and tumor cells. NGR peptides are useful for preparing anticancer agents by delivering cytotoxic drugs, proapoptotic peptides, and TNF to the tumor vasculature.<sup>3</sup> The tumor-homing characteristic can be used in radiotherapy that relies on  $\beta^-$  particle decay.

Ma W<sup>51</sup> designed a novel fusion NGR-VEGI protein and labeled it with Rhenium-188 ( $^{188}\text{Re}$ ) for SPECT tumor imaging and tumor therapy in mice bearing human fibrosarcoma HT-1080 xenografts. The goal of the fusion protein was to increase the tumor specificity of vascular endothelial growth inhibitor (VEGI). The VEGI is a member of the TNF family and is correlated with lower tumor recurrence, longer survival time, and better prognosis in patients with breast cancer. It can activate multiple signaling pathways and inhibit endothelial cell proliferation, angiogenesis, and tumor growth. In tandem with

NGR peptides, it could improve the tumor specificity and reduce adverse side effects of VEGF.<sup>52,53</sup> Here,  $^{188}\text{Re}$  ( $T_{1/2} = 16.98$  hours) could emit  $\gamma$ -rays for radioimaging and  $\beta^-$  particles for radiotherapy. The biodistribution study suggested relatively good radioactivity in tumor ( $1.66\% \pm 0.32\%$  ID/g) and good tumor to muscle ratio ( $4.98 \pm 0.25$ ) of  $^{188}\text{Re}$ -NGR-VEGF at 24 hours. The in vivo radiotherapy effect indicated that 18.5 MBq of  $^{188}\text{Re}$ -NGR-VEGF obviously inhibits tumor growth in HT-1080 tumor-bearing mice versus saline, NGR treatment, and NGR-VEGF treatment alone. No toxicity was observed, which concurs with the in vitro inhibitory effect. The results demonstrated that  $^{188}\text{Re}$ -NGR-VEGF can significantly induce HT-1080 tumor cell death. However, HT-1080 tumor growth slowly recurred after 18 days of treatment due to the relatively short half-life of  $^{188}\text{Re}$ . This could be solved by replacing  $^{188}\text{Re}$  with longer half-life radionuclides such as  $^{177}\text{Lu}$  ( $T_{1/2} = 6.7$  days) and  $^{90}\text{Y}$  ( $T_{1/2} = 2.7$  days) or multiple administration.

Vats K et al<sup>54</sup> evaluated the potential of  $^{177}\text{Lu}$ -labeled carbon nanospheres (CNS) as nano radiopharmaceuticals for molecular imaging and therapy. Carbon nanospheres are composed of the nontoxic carbon and have been broadly explored in the field of cancer nanomedicine. Their small size, large surface area, spherical shape, and reactive functionalities of CNS lead to high biocompatibility and facile chemical conjugation. They can be tagged with targeting vectors (peptides or antibodies), chemotherapeutic drugs, or imaging entities (dyes or radioisotopes) to combine diagnostic and therapeutic modalities in a single nanoplatform. Furthermore, enhanced surface reactivity can also facilitate multimeric nanosphere systems with multivalent displays of ligands (peptides/drugs) to amplify the concentration at the target and improve its specificity. According to the biodistribution studies, the  $^{177}\text{Lu}$ -labeled nanosphere-peptide conjugate  $^{177}\text{Lu}$ -DOTA-CNS-cNGR exhibited 2.3-fold higher tumor accumulation than  $^{177}\text{Lu}$ -DOTA-cNGR (without CNS); however, this was lower than  $^{177}\text{Lu}$ -DOTA-CNS without the peptide. Rapid clearance of  $^{177}\text{Lu}$ -DOTA-CNS-G3-cNGR resulted in significantly higher tumor to blood and tumor to muscle ratios versus  $^{177}\text{Lu}$ -DOTA-cNGR and  $^{177}\text{Lu}$ -DOTA-CNS. These results suggested that CNS combined with NGR peptides form an important part of the targeted radio-nanoprobes in the future.

## NGR-Based Cardiovascular Radio Imaging

Angiogenesis is a natural repair process in some nonmalignant diseases such as myocardial ischemia, cerebrovascular infarction, and arthritis. RGD peptides can have high tracer uptake in the myocardial infarction.<sup>47</sup> CD13 is also expressed on fibroblasts and inflammatory cells in acute myocardial ischemia. Tillmanns J<sup>55</sup> proved that uptake of  $^{68}\text{Ga}$ -NOTA-cNGR was correlated with fibroblast and inflammatory cell infiltration in the infarcted myocardium as well as  $^{68}\text{Ga}$ -NOTA-cRGD uptake. The results also revealed that radiolabeled NGR tracers could be used for in vivo imaging of the early wound-healing phase after myocardial infarction.

Radiolabeled monomeric cyclic peptide cyclo (Cys-Asn-Gly-Arg-Gly) (coNGR) and its tetramer co(NGR)<sub>4</sub> can be cyclized by native chemical ligation instead of disulfide bridging. Both coNGR-based imaging agents displayed considerably higher SUVs at infarcted areas. Uptake patterns of  $^{111}\text{In}$ -coNGR and  $^{111}\text{In}$ -co(NGR)<sub>4</sub> were coincident with CD13 immunohistochemistry on excised hearts. Here, Co(NGR)<sub>4</sub> displayed a significantly higher specific uptake in infarcted myocardium versus coNGR. These studies show that NGR could be a promising sensitive imaging agent for the detection of angiogenesis in infarcted myocardium.<sup>56</sup>

## Optical Imaging

NGR-labeled with small molecular fluorophores, quantum dot (QDs), and polymer carriers are widely used methods for optical molecular imaging. Both linear and cyclized NGR peptide can be coupled to a maleimide-modified fluorescent dye Oregon Green 488 (OG488) for optical imaging. In CD13-positive tumor cells, the affinity of OG488 cyclic KNGRE is 3.6-fold higher than that of OG488 linear KNGRG.<sup>16</sup> In addition to OG488 dye, NGR can also be coupled to the fluorescent dye Cy5.5 for optical imaging. Despite the CD13-positive HT-1080 tumor region exhibiting specific accumulation of cNGR-Cy5.5, the overaccumulation of cNGR-Cy5.5 in the kidney and liver can reduce the sensitivity to tumors.<sup>16,17</sup>

Compared to traditional dyes, QDs emission is brighter with narrow emission spectra and is tunable based on its size. Moreover, QD's optical performance is more stable and durable.<sup>57</sup> cNGR has been combined with OG488 or biotin, and the complex was assessed in a CD13-positive murine endothelial cell line. The biotin-tagged NGR multivalently labeled the QDs, which gave the cNGR-QDs greater intensity and more persistent fluorescence than the cNGR-OG488 dye. In vivo fluorescence microscopy revealed the lower bleaching rate and higher intrinsic fluorescence of QD versus OG488 dye. Thus, the cNGR-QD strongly labeled CD13-rich cells. However, new generations of less toxic and more easily cleared QDs are needed.<sup>58</sup>

Direct conjugation suffers from a low signal/background ratio and in vivo stability of peptides and fluorophores. They can be conjugated to a polymeric carrier such as liposomes that can be encapsulated with multiple probes to produce amplified signals for imaging. Taking advantage of the intrinsic fluorescence properties of DOX, DOX-encapsulated NGR-modified liposome showed a 10-fold enhancement in affinity for CD13-positive cancer cells versus NGR peptide alone.<sup>59</sup> Other fluorescent studies of NGR peptides include fluorescein isothiocyanate (FITC)-labeled N-(hydroxypropyl)methacrylamide copolymer, FITC-labeled cytoskeletal proteins actin, and 1,1'-dioctadecyl-3,3',3'-tetramethylindocarbocyanine perchlorate (DiI)-labeled biodegradable di-block copolymer; PEG-poly (D, L-lactide) also showed promising results for tumor imaging.<sup>16,17</sup>



## Conclusion

Peptides containing the NGR motif have been used as a homing agent for delivery of therapeutics, cytokines, peptides, chemicals, liposomes, and polymeric micelles to activated tumor neovascular tissue. This strategy can enhance therapeutic efficacy and reduce systemic toxicity. Various radiolabeled NGR peptides with different molecular scaffolds and chelators exhibit great differences in affinity, specificity, and pharmacokinetics. Dimerizing NGR peptides is a promising strategy to improve pharmacokinetic characteristics and tumor to nontarget ratio. Moreover, the different stability and receptor-binding specificity caused by different molecular scaffolds should be carefully considered. Generally speaking, cNGR displayed a stronger affinity and higher specificity toward the CD13 receptors versus linear ones.  $^{68}\text{Ga}$ -labeled dimeric compounds could be the most ideal radioactive probes so far and can greatly reduce liver uptake with comparable tumor uptake as  $^{64}\text{Cu}$  and  $^{99\text{m}}\text{Tc}$ . The use of radiolabeled NGR peptides for imaging of CD13 expression has good potential for tumor imaging and therapy.

## Declaration of Conflicting Interests

The author(s) declared no potential conflicts of interest with respect to the research, authorship, and/or publication of this article.

## Funding

The author(s) received no financial support for the research, authorship, and/or publication of this article.

## ORCID iD

Liqing Zhu  <https://orcid.org/0000-0003-0844-985X>

## References

- Wickstrom M, Larsson R, Nygren P, Gullbo J. Aminopeptidase N (CD13) as a target for cancer chemotherapy. *Cancer Sci*. 2011; 102(3):501–508.
- Renata P, Erkki K, Renate K, et al. Aminopeptidase N is a receptor for tumor-homing peptides and a target for inhibiting angiogenesis 1. *Cancer Res*. 2000;60(3):722–727.
- Angelo C, Curnis F. Tumor vasculature targeting through NGR peptide-based drug delivery systems. *Curr Pharm Biotechnol*. 2011;12(8):1128–1134.
- Flavio C, Anna G, Angelina S, Cattaneo A, Magni F, Corti A. Targeted delivery of IFN $\gamma$  to tumor vessels uncouples antitumor from counterregulatory mechanisms. *Cancer Res*. 2005;65(7):2906–2913.
- Corti A, Curnis F, Arap W, Pasqualini R. The neovasculature homing motif NGR: more than meets the eye. *Blood*. 2008; 112(7):2628–2635.
- Wadih A, Renata P, Ruoslahti E. Cancer treatment by targeted drug delivery to tumor vasculature in a mouse model. *Science*. 2016;279(5349):377–380.
- Colombo G, Curnis F, De Mori GMS, et al. Structure-activity relationships of linear and cyclic peptides containing the NGR tumor-homing motif. *J Biol Chem*. 2002;277(49):47891–47897.
- Ayele HN, Jenna LM, Goutham R, Drake SK, Wood BJ, Dreher MR. Synthesis and in vitro evaluation of cyclic NGR peptide targeted thermally sensitive liposome. *J. Control Release* 2010; 143(2):265–273.
- Metaferia BB, Rittler M, Gheeya JS, et al. Synthesis of novel cyclic NGR/RGD peptide analogs via on resin click chemistry. *Bioorg Med Chem Lett*. 2010;20(24):7337–7340.
- Xie X, Yang Y, Yang Y, Zhang H, Li Y, Mei X. A photo-responsive peptide- and asparagine-glycine-arginine (NGR) peptide-mediated liposomal delivery system. *Drug Deliv*. 2016; 23(7):2445–2456.
- Curnis F, Cattaneo A, Longhi R, et al. Critical role of flanking residues in NGR-to-isoDGR transition and CD13/integrin receptor switching. *J Biol Chem*. 2010;285(12):9114–9123.
- Kirikoshi R, Manabe N, Takahashi O. Succinimide formation from an NGR-containing cyclic peptide: computational evidence for catalytic roles of phosphate buffer and the arginine side chain. *Int J Mol Sci*. 2017;18(2):429. doi:10.3390/ijms18020429
- Yang Y, Yang Y, Xie X, et al. PEGylated liposomes with NGR ligand and heat-activable cell-penetrating peptide-doxorubicin conjugate for tumor-specific therapy. *Biomaterials*. 2014; 35(14):4368–4381.
- Seidi K, Jahanban ER, Monhemi H, et al. NGR (Asn-Gly-Arg)-targeted delivery of coagulase to tumor vasculature arrests cancer cell growth. *Oncogene*. 2018;37(29):3967–3980.
- Persigehl T, Ring J, Bremer C, et al. Non-invasive monitoring of tumor-vessel infarction by retargeted truncated tissue factor (tTF-NGR) using multi-modal imaging. *Angiogenesis*. 2014;17(1):235–246.
- Rongsheng EW, Youhong N, Haifan W, Amin MN, Cai J. Development of NGR peptide-based agents for tumor imaging. *Am J Nucl Med Mol Imaging*. 2011;1(1):36–46.
- Rongsheng EW, Youhong N, Haifan W, Hu Y, Cai J. Development of NGR-based anti-cancer agents for targeted therapeutics and imaging. *Anticancer Agents Med Chem*. 2012;12(1):76–86.
- Di Matteo P, Mangia P, Tiziano E, et al. Anti-metastatic activity of the tumor vascular targeting agent NGR-TNF. *Clin Exp Metastasis*. 2015;32(3):289–300.
- Corti A, Curnis F, Rossoni G, Marcucci F, Gregorc V. Peptide-mediated targeting of cytokines to tumor vasculature: the NGR-hTNF example. *BioDrugs*. 2013;27(6):591–603.
- van Laarhoven HWM, Fiedler W, Desar IME, et al. Phase I clinical and cognitive resonance imaging study of the vascular agent NGR-hTNF in patients with advanced cancers (European Organization for Research and Treatment of Cancer Study 16041). *Clin Cancer Res*. 2010;16(4):1315–1323.
- Gregorc V, Citterio G, Vitali G, et al. Defining the optimal biological dose of NGR-hTNF, a selective vascular targeting agent, in advanced solid tumours. *Eur J Cancer*. 2010;46(1):198–206.
- Gregorc V, Gaafar RM, Favaretto A, et al. NGR-hTNF in combination with best investigator choice in previously treated malignant pleural mesothelioma (NGR015): a randomised, double-blind, placebo-controlled phase 3 trial. *Lancet Oncol*. 2018;19(6):799–811.

23. Gregorc V, Cavina R, Novello S, et al. NGR-hTNF and doxorubicin as second-line treatment of patients with small cell lung cancer. *Oncologist*. 2018;23(10):1133–e1112.
24. Parmiani G, Pilla L, Corti A, et al. A pilot phase I study combining peptide-based vaccination and NGR-hTNF vessel targeting therapy in metastatic melanoma. *OncoImmunology*. 2014;3(11):e963406.
25. Lorusso D, Scambia G, Amadio G, et al. Phase II study of NGR-hTNF in combination with doxorubicin in relapsed ovarian cancer patients. *Br J Cancer*. 2012;107(1):37–42.
26. Mammoliti S, Andretta V, Bennicelli E, et al. Two doses of NGR-hTNF in combination with capecitabine plus oxaliplatin in colorectal cancer patients failing standard therapies. *Ann Oncol*. 2010;22:973–978.
27. Santoro A, Pressiani T, Citterio G, et al. Activity and safety of NGR-hTNF, a selective vascular-targeting agent, in previously treated patients with advanced hepatocellular carcinoma. *Br J Cancer*. 2010;103(6):837–844.
28. Zhang J, Lu X, Wan N, et al. <sup>68</sup>Ga-DOTA-NGR as a novel molecular probe for APN-positive tumor imaging using MicroPET. *Nucl Med Biol*. 2014;41(3):268–275.
29. He YX, Guo QY. Clinical applications and advances of positron emission tomography with fluorine-18-fluorodeoxyglucose <sup>18</sup>F-FDG in the diagnosis of liver neoplasms. *Postgrad Med J*. 2008;84(991):246–251.
30. Gao Y, Wang Z, Ma X, et al. The uptake exploration of <sup>68</sup>Ga-labeled NGR in well-differentiated hepatocellular carcinoma xenografts: Indication for the new clinical translational of a tracer based on NGR. *Oncol Rep*. 2017;38(5):2859–2866.
31. Ramogida CF, Orvig C. Tumour targeting with radiometals for diagnosis and therapy. *Chem Commun*. 2013;49(42):4720–4739.
32. Shao Y, Liang W, Kang F, et al. <sup>68</sup>Ga-labeled cyclic NGR peptide for microPET imaging of CD13 receptor expression. *Molecules*. 2014;19(8):11600–11612.
33. Werle M, Bernkop-Schnürch A. Strategies to improve plasma half life time of peptide and protein drugs. *Amino Acids*. 2006;30(4):351–367.
34. Zhao M, Yang W, Zhang M, et al. Evaluation of <sup>68</sup>Ga-labeled iNGR peptide with tumor-penetrating motif for microPET imaging of CD13-positive tumor xenografts. *Tumour Biol*. 2016;37(9):12123–12131.
35. Luca A, Lise R, Kazuki NS, et al. De novo design of a tumor-penetrating peptide. *Cancer Res*. 2013;73(2):804–812.
36. Ma W, Wang Z, Yang W, Ma X, Kang F, Wang J. Biodistribution and SPECT imaging study of <sup>99m</sup>Tc labeling NGR peptide in nude mice bearing human HepG2 hepatoma. *Biomed Res Int*. 2014;2014:618096.
37. Faintuch BL, Oliveira EA, Targino RC, Moro AM. Radiolabeled NGR phage display peptide sequence for tumor targeting. *Appl Radiat Isot*. 2014;86:41–45.
38. Kim DW, Kim WH, Kim MH, Kim CG. Novel Tc-99m labeled ELR-containing 6-mer peptides for tumor imaging in epidermoid carcinoma xenografts model: a pilot study. *Ann Nucl Med*. 2013;27(10):892–897.
39. Kim DW, Kim WH, Kim MH, Kim CG. Synthesis and evaluation of novel <sup>99m</sup>Tc labeled NGR-containing hexapeptides as tumor imaging agents. *J Labelled Comp Radiopharm*. 2015;58(2):30–35.
40. Ma W, Kang F, Wang Z, et al. <sup>99m</sup>Tc-labeled monomeric and dimeric NGR peptides for SPECT imaging of CD13 receptor in tumor-bearing mice. *Amino Acids*. 2013;44(5):1337–1345.
41. Vats K, Satpati D, Sharma R, et al. <sup>99m</sup>Tc-labeled NGR-chlorambucil conjugate, <sup>99m</sup>Tc-HYNIC-CLB-c(NGR) for targeted chemotherapy and molecular imaging. *J Labelled Comp Radiopharm*. 2017;60(9):431–438.
42. Millard M, Gallagher JD, Olenyuk BZ, Neamati N. A selective mitochondrial-targeted chlorambucil with remarkable cytotoxicity in breast and pancreatic cancers. *J Med Chem*. 2013;56(22):9170–9179.
43. Gaertner FC, Kessler H, Wester HJ, Schwaiger M, Beer AJ. Radiolabelled RGD peptides for imaging and therapy. *Eur J Nucl Med Mol Imaging*. 2012;39(1):126–138.
44. Chen K, Ma W, Li G, et al. Synthesis and evaluation of <sup>64</sup>Cu-labeled monomeric and dimeric NGR peptides for microPET imaging of CD13 receptor expression. *Mol Pharm*. 2013;10(1):417–427.
45. Li G, Wang X, Zong S, Wang J, Conti PS, Chen K. MicroPET imaging of CD13 expression using a <sup>64</sup>Cu-labeled dimeric NGR peptide based on sarcophagine cage. *Mol Pharm*. 2014;11(11):3938–3946.
46. Shao Y, Liang W, Kang F, et al. A direct comparison of tumor angiogenesis with <sup>68</sup>Ga-labeled NGR and RGD peptides in HT-1080 tumor xenografts using microPET imaging. *Amino Acids*. 2014;46(10):2355–2364.
47. Eo JS, Jeong JM. Angiogenesis imaging using <sup>68</sup>Ga-RGD PET/CT: therapeutic implications. *Semin Nucl Med*. 2016;46(5):419–427.
48. Mate G, Kertesz I, Enyedi KN, et al. In vivo imaging of aminopeptidase N (CD13) receptors in experimental renal tumors using the novel radiotracer <sup>68</sup>Ga-NOTA-c(NGR). *Eur J Pharm Sci*. 2015;69:61–71.
49. Oliveira EA, Faintuch BL, Nunez EG, et al. Radiotracers for different angiogenesis receptors in a melanoma model. *Melanoma Res*. 2012;22(1):45–53.
50. Satpati D, Sharma R, Kumar C, et al. <sup>68</sup>Ga-Chelation and comparative evaluation of N, N'-bis-[2-hydroxy-5-(carboxyethyl)-benzyl]ethylenediamine-N, N'-diacetic acid (HBED-CC) conjugated NGR and RGD peptides as tumor targeted molecular imaging probes. *MedChemComm*. 2017;8(3):673–679.
51. Ma W, Shao Y, Yang W, et al. Evaluation of <sup>188</sup>Re-labeled NGR-VEGI protein for radioimaging and radiotherapy in mice bearing human fibrosarcoma HT-1080 xenografts. *Tumour Biol*. 2016;37(7):9121–9129.
52. Haridas V, Shrivastava A, Su J, et al. VEGI, a new member of the TNF family activates nuclear factor-κB and c-Jun N-terminal kinase and modulates cell growth. *Oncogene*. 1999;18(47):6496–6504.
53. Parr C, Gan CH, Watkins G, Jiang WG. Reduced vascular endothelial growth inhibitor (VEGI) expression is associated with poor prognosis in breast cancer patients. *Angiogenesis*. 2006;9(2):73–81.
54. Vats K, Satpati AK, Sharma R, Sarma HD, Satpati D, Dash A. <sup>177</sup>Lu-labeled cyclic Asn-Gly-Arg peptide tagged carbon

- nanospheres as tumor targeting radio-nanoprobes. *J Pharm Biomed Anal.* 2018;152:173–178.
55. Tillmanns J, Schneider M, Fraccarollo D, et al. PET imaging of cardiac wound healing using a novel  $^{68}\text{Ga}$ -labeled NGR probe in rat myocardial infarction. *Mol Imaging Biol.* 2015; 17(1):76–86.
56. Hendrikx G, Hackeng TM, van Gorp R, et al. Use of cyclic backbone NGR-Based SPECT to increase efficacy of postmyocardial infarction angiogenesis imaging. *Contrast Media Mol Imaging.* 2017;2017:8638549.
57. Walling MA, Novak JA, Shepard JR. Quantum dots for live cell and in vivo imaging. *Int J Mol Sci.* 2009;10(2):441–491.
58. Buehler A, van Zandvoort MA, Stelt BJ, et al. cNGR: a novel homing sequence for CD13/APN targeted molecular imaging of murine cardiac angiogenesis in vivo. *Arterioscler Thromb Vasc Biol.* 2006;26(12):2681–2687.
59. Garde SV, Forté AJ, Ge M, et al. Binding and internalization of NGR-peptide-targeted liposomal doxorubicin (TVT-DOX) in CD13-expressing cells and its antitumor effects. *Anticancer Drugs.* 2007;18(10):1189–1200.